Title

An updated staging system for cephalochordate development: one table suits them all

Authors

João E. Carvalho[1#], François Lahaye[1], Luok Wen Yong[2], Jenifer C. Croce[1], Hector Escrivá[3], Jr-Kai Yu[2], Michael Schubert[1]*

Affiliations

1- Sorbonne Université, CNRS, Laboratoire de Biologie du Développement de Villefranche-sur-Mer, Institut de la Mer de Villefranche, Villefranche-sur-Mer, France

2- Institute of Cellular and Organismic Biology, Academia Sinica, Taipei, Taiwan

3- Sorbonne Université, CNRS, Biologie Intégrative des Organismes Marins, Observatoire Océanologique, Banyuls-sur-Mer, France

Current address: Institute for Research on Cancer and Aging, Nice (IRCAN), CNRS, INSERM, Université Côte d'Azur, Nice, France

* Corresponding author

Abstract

Background: The chordates are divided into three subphyla: Vertebrata, Tunicata and Cephalochordata. Phylogenetically, the Cephalochordata, more commonly known as lancelets or amphioxus, constitute the sister group of Vertebrata plus Tunicata. Due to their phylogenetic position and their conserved morphology and genome architecture, lancelets are important models for understanding the evolutionary history of chordates. Lancelets are small, marine filter-feeders, and the few dozen species that have so far been described have been grouped into three genera: *Branchiostoma*, *Epigonichthys* and *Asymmetron*. Given their relevance for addressing questions about the evolutionary diversification of chordates, lancelets have been the subjects of study by generations of scientists, with the first descriptions of adult anatomy and developmental morphology dating back to the 19th century. Today, several different lancelet species are used as laboratory models, predominantly for developmental, molecular and genomic studies. It is thus very surprising that there is currently no universal staging system and no unambiguous nomenclature for developing lancelets.

Results: We illustrated the development of the European amphioxus (*Branchiostoma lanceolatum*) using confocal microscopy and compiled a streamlined developmental staging system, from fertilization through larval life, with an unambiguous stage nomenclature. By tracing growth curves of the European amphioxus reared at different temperatures, we were able to show that our staging system permits the easy conversion of any developmental time into a defined

stage name. Furthermore, comparisons of embryos and larvae from the European amphioxus (*B. lanceolatum*), the Florida amphioxus (*B. floridae*), the Chinese amphioxus (*B. belcheri*), the Japanese amphioxus (*B. japonicum*) and the Bahamas lancelet (*Asymmetron lucayanum*) demonstrated that our staging system can readily be applied to other lancelet species.

Conclusions: Here, we propose an updated staging and nomenclature system for lancelets. Although the detailed staging description was carried out on developing *B. lanceolatum*, comparisons with other lancelet species strongly suggest that both staging and nomenclature are applicable to all extant lancelets. We thus believe that this description of embryonic and larval development can be of great use for the scientific community and hope that it will become the new standard for defining and naming developing lancelets.

Keywords

Amphioxus, *Asymmetron lucayanum, Branchiostoma belcheri, Branchiostoma floridae, Branchiostoma japonicum, Branchiostoma lanceolatum,* Confocal Microscopy, Embryonic and Larval Development, Evolution and Development, Lancelet

Background

The subphylum Cephalochordata comprises only a few dozen species of small, lancet-shaped filter-feeders [1,2]. The Cephalochordata (commonly referred to as lancelets or amphioxus) belong to the chordate phylum and are the sister group to all other chordates (Tunicata plus Vertebrata) [1,2]. Due to this phylogenetic position and their slow evolutionary rate [3], lancelets are considered valuable proxies for the chordate ancestor, both at the anatomic and genomic levels [1,2]. The subphylum Cephalochordata is subdivided into three genera: *Branchiostoma*, *Epigonichthys* and *Asymmetron* [4–11]. Recent analyses of mitochondrial genomes suggested that the genus *Asymmetron* occupies the basal position and diverged from the *Epigonichthys* plus *Branchiostoma* clade about 42 Mya (million years ago). It was further proposed that the split of the *Epigonichthys* and *Branchiostoma* lineages occurred about 36 Mya [12] and that speciation within the genus *Branchiostoma* took place between 28 and 22 Mya [12].

The importance of lancelets for understanding chordate evolution has driven generations of scientists to study their embryos and larvae [13]. An initial description of lancelet development was thus already performed in the 19th century, on *B. lanceolatum* material obtained in Naples, Italy [14]. This work was subsequently completed, at the end of the 19th and the beginning of the 20th century, by a series of additional surveys on the same species [15–17]. More recently, in the early 1990s, the early development of *B. japonicum* has been the subject of a detailed characterization by electron microscopy [18–20]. A similar approach has been used to characterize neurulae, larvae and post-metamorphic

specimens of *B. floridae* [21]. The most recent description of lancelet development was that of *A. lucayanum* embryos and larvae using differential interference contrast (DIC) microscopy [5,22]. Taken together, these studies have revealed that the ontogeny of lancelets is a highly coordinated and conserved process. It is thus all the more surprising that there is currently no universal developmental staging system available for the members of this subphylum.

In the course of the last three decades, lancelets have become important models for addressing developmental processes from a molecular and genomic perspective [2,4,23–25]. However, unlike for other developmental model organisms, such as fruit flies or zebrafish, the scientific community is using different lancelet species for their studies [4]. Husbandry protocols have been established for at least five lancelet species [4], and, due to the absence of a universal staging system, the naming of embryos and larvae obtained with these protocols has become extremely confusing. While developing lancelets are often named in accordance with previous reports on the same species [1,26–28], it is also not uncommon to indicate the time after fertilization, usually measured in hours, although developmental speed is known to vary between lancelet species and to depend on the rearing temperature, which is not the same in each study [2,29]. This lack of an unambiguous nomenclature for developing lancelets artificially complicates comparisons of results obtained in different species and sometimes even within the same species, for example, when two laboratories use incompatible staging styles [28,30]. There is therefore an urgent need to establish an easy and systematic classification for embryonic and larval development that applies to different lancelet species.

To achieve this objective, we illustrated the development of *B. lanceolatum* using confocal microscopy and compared embryos and larvae from this species with those of other lancelets. By applying the stage definitions of Hirakow and Kajita [18–20] and Lu and colleagues [26] to *B. lanceolatum* development, we compiled a streamlined staging system, from fertilization through larval life, with an unambiguous stage nomenclature. Comparisons between *B. lanceolatum*, *B. floridae*, *B. belcheri*, *B. japonicum* and *A. lucayanum* embryos and larvae demonstrated that this updated staging system can readily be applied to other lancelet species. We hope that the scientific community will widely adopt this universal developmental staging system to facilitate the use of different lancelets as laboratory models.

Results

Making use of the available *in vitro* culture protocols for developing lancelets [4], *B. lanceolatum* embryos and larvae were reared at constant temperatures and fixed at the desired stages. Prior to confocal imaging, embryos and larvae were labeled with fluorescent probes marking cell membranes and nuclei, hence allowing detailed anatomical analyses of individual developmental stages. In the following, each stage of the updated staging system will be presented and defined. We further provide information on the development of *B. lanceolatum* at different temperatures, based on the differential addition of somite pairs over time. Finally, to demonstrate the universality of the updated staging system, we compare *B.*

lanceolatum embryos and larvae with those from four other lancelet species: *B. floridae*, *B. belcheri*, *B. japonicum* and *A. lucayanum*.

Fertilization and cleavage

The mature lancelet oocyte undergoes the first meiotic division with formation of the first polar body and is subsequently arrested in the second meiotic metaphase [31]. The second meiotic division of the oocyte is completed within 10 min following fertilization, leading to the formation of the second polar body and the migration of the maternal chromosomes to the animal pole of the 1-cell stage (Fig. 1A) [32]. The 1-cell stage is semi-opaque, due to the high quantity of granules uniformly distributed throughout the cell, and is surrounded by a membrane called the vitelline layer [33]. The sperm can enter the oocyte anywhere, but will preferentially do so in the vegetal hemisphere [32]. Independent of the entry point, the nucleus of the sperm will first migrate to the vegetal half and will only then join the maternal chromosomes at the animal pole [1]. Very soon after fertilization, a whorl composed of sheets of endoplasmic reticulum is formed within the 1-cell stage. This whorl likely constitutes the germ plasm, since expression of the germ cell markers, such as *nanos* and *vasa*, is associated with this structure [34]. As soon as fertilization occurs, the vitelline layer detaches from the body of the 1-cell stage and expands, giving rise to the fertilization envelope [35]. Cleavage, gastrulation and the first stages of neurulation occur within the fertilization envelope [1].

Lancelet cleavage is radial holoblastic. The first cleavage starts from the animal pole (identifiable by the position of the polar body) and gives rise to

identically-shaped blastomeres, the 2-cell stage (Fig. 1B). Each one of the first two blastomeres can give rise to a complete animal, but only one of the two blastomeres will inherit the germ plasm [31]. The second division is meridional and at a right angle to the first one, creating four identical blastomeres, the 4-cell stage (Fig. 1C). Individual blastomeres are not adhering very strongly at this stage, and their dissociation can lead to the formation of twins or even quadruplets. Cleavage continues by an equatorial division, creating four animal and four vegetal blastomeres at the 8-cell stage, with the former being smaller than the latter (Fig. 1D). The blastomeres are held together by short microvilli and slender filopodial processes that bridge the space between adjacent blastomeres (insets in Fig. 1D,E) [18]. The 16-cell stage is the result of a meridional cleavage (Fig. 1E), and the 32-cell stage of a subsequent equatorial cleavage of each blastomere (Fig. 1F). At this stage, the embryo is composed of a single layer of cells forming a central cavity called the blastocoel [18,36]. The blastomeres will keep dividing regularly, hence giving rise initially to the 64-cell stage (Fig. 1G) and subsequently to the 128-cell stage (Fig. 1H). The 8th cell division cycle is characterized by the initiation of asynchronous cell divisions within the embryo [18,36], which also marks the completion of blastula formation at the B stage (Fig. 1I).

Gastrulation

The cells forming the hollow blastula are not identical in shape and size. The vegetal blastula cells are larger and hence indicate the location of the initial flattening of the gastrula at the G0 stage (Fig. 2A) [1,33]. The vegetal side of the embryo will subsequently flatten at the G1 stage (Fig. 2B,B') and start to invaginate

into the blastocoel at the G2 stage, hence forming a depression at the vegetal side of the embryo (Fig. 2C,C') [19]. The cells invaginating into the blastocoel correspond to the presumptive endomesoderm, while the non-invaginating cells of the outer layer constitute the future general and neural ectoderm [31]. As gastrulation proceeds, the ingressing cells reduce the size of the blastocoelic cavity, ultimately leading, at the G3 stage, to a two-layered gastrula with an archenteron and a blastoporal lip. In this cap-shaped gastrula, the diameter of the blastopore is about half the size of the embryo (Fig. 2D,D') [19]. Subsequent gastrulation movements result in an expansion of the cavity of the archenteron and in a narrowing of the blastoporal opening, which, in turn, inflects the blastoporal lip, forming a cup-shaped gastrula at the G4 stage (Fig. 2E,E') and a vase-shaped gastrula at the G5 stage (Fig. 2F,F') [19]. Starting at the G5 stage, differences between the dorsal and ventral sides of the embryo become discernable, with the dorsal side beginning to flatten (Fig. 2F,F') [33]. These differences become more pronounced at the G6 stage, as the size of the blastopore continues to decrease and the embryo commences to elongate (Fig. 2G,G'). At this late gastrula stage, the embryo is bottle-shaped, and the blastopore starts to incline towards the dorsal side of the embryo, which is likely a chordate synapomorphy [33].

Expression patterns of marker genes, such as *hox1*, *hox3*, *otx* and *foxq2*, have determined that, with the exception of the tissues located in the immediate vicinity of the blastopore, most of the gastrula is destined to become the head. This includes the lancelet brain homolog, the anteriormost somites, the pharynx with mouth and gill slits as well as the anterior section of the notochord [31]. Transplantation experiments further suggest that the dorsal lip of the blastopore

corresponds to a gastrulation organizer, similar or equivalent to the Spemann-Mangold organizer of vertebrates [37,38]. This notion is supported by the expression of homologs of Spemann's organizer genes, such as *nodal*, *lefty* and *chordin*, in the dorsal lip of the lancelet blastopore [39,40]. Accordingly, exogenous BMP4 induces the loss of the lancelet notochord and neural tube, and the upregulation of Nodal signaling converts the lancelet ectoderm to neuroectoderm [31,39,40].

Neurulation

Following gastrulation, all ectodermal cells develop cilia and the embryo subsequently starts to rotate within the fertilization envelope by ciliary movement [1,26]. At this point in development, neurulation starts. The embryo is unsegmented and shows a typical dipoblastic organization, with the ectoderm externally and the endomesoderm internally (Fig. 3A). At this N0 stage, a small blastopore is still visible and the dorsal ectoderm, destined to become the neuroectoderm, is flat with a shallow longitudinal groove (Fig. 3A). The subsequent N1 stage is characterized by the establishment of the first somites (somite pairs 1 through 3) (Fig. 3B). The mesoderm, located dorsally within the endomesoderm, starts forming three folds, one medially that will develop into the notochord and two dorso-laterally that will give rise to the anterior somites that, at the N1 stage, will start pinching off in an anterior to posterior sequence. At the same stage, the dorsal non-neural ectoderm starts to dissociate from the neural plate. Following dissociation, the ectodermal cells will migrate over the neural plate using lamellipodia and fuse at the dorsal midline. At the end of this process, the neural plate will be completely covered by

non-neural ectoderm, and the neuropore will have been formed anteriorly [17,31,41].

As neurulation proceeds, the archenteron is no longer in contact with the exterior, but still communicates with the forming neural tube: the blastopore is incorporated into the neurenteric canal, which connects the neural tube with the archenteron, which becomes the presumptive gastric cavity [33]. The embryo keeps elongating by the addition of new somites, reaching 4 to 5 somite pairs at the N2 stage (Fig. 3C,C'). At this stage, the embryo hatches from the fertilization envelope by the synthesis and secretion of hatching enzymes and starts swimming freely by ciliary activity [21,42]. The neural plate is V-shaped and the primordium of the notochord is a round mass of cells extending ventrally under the neural plate. Central nervous system, notochord and somites are thus clearly discernable at this stage, although the boundaries between notochord and somites are not always evident (Fig. 3C') [20].

At the N3 stage, the embryo is characterized by 6 to 7 somite pairs (Fig. 3D,D'). The neural tube is closing, but will only become circular at subsequent developmental stages (Fig. 3D,D'). The notochord is individualized from the somites, except at the most anterior tip of the embryo [16,17]. Ventral extensions of the somites start to generate the lateral and ventral coeloms as well as the musculature of the atrial floor [31]. Furthermore, expression of early markers of Hatschek's nephridium, such as *pax2/5/8*, becomes detectable in the mesothelial wall of the first somite on the left side of the embryo [43–45]. The archenteron located anterior to the first somite pair starts expanding, forming two dorso-lateral lobes. Subsequently, at the N4 stage, which is characterized by 8 to 9 somite pairs,

the asymmetric formation of somites from the tail bud is initiated (Fig. 3E,E'). Thus, while early somitogenesis occurs by enterocoely from endomesoderm internalized during gastrulation, starting at the N4 stage, somites are formed by schizocoely from the tail bud [1]. In the anterior archenteron, the two dorso-lateral lobes have formed two distinctive head cavities: Hatschek's left and right diverticulum [33,36].

The N5 stage is characterized by 10 to 11 somite pairs (Fig. 3F,F'). The left and right diverticula are now asymmetrically organized. While the left diverticulum roughly maintains its original form and size, the right diverticulum moves anteriorly, flattens and increases its size [33]. At this stage, the primordium of the club shaped gland is first discernable, ventrally in the anterior endoderm on the right side of the embryo. This developmental stage is further characterized by a decrease of proliferative activity in somites and notochord, where it becomes limited to the posterior end. However, cell proliferation continues in the tail bud, in the endoderm and in the anterior neural plate [46].

Tailbud and larva

Following neurulation, the embryo has a tailbud-like shape with 12 pairs of somites and exhibits a transitional morphology between neurula and larva stages (Fig. 4A,A'). At this T0 stage, the anterior portion of the embryo becomes clearly distinct from the posterior one, as the pharyngeal region commences to grow. In addition, the embryo starts to twitch and bend as its neuromuscular system slowly becomes operational [20]. Consequently, embryos at the subsequent T1 stage are longer than at the T0 stage, and this length difference is not due to the addition of a significant number of new somite pairs, but to the maturation of the existing ones

(Fig. 4B,B'). The overall shape of the embryo also changes at the T1 stage. As the body elongates, it is becoming more slender, a distinctive rostral snout is appearing and the caudal ectodermal starts forming a tail fin [20]. The first pigment spot in the central nervous system appears, located in the ventral wall of the neural tube at the level of the fifth somite pair [33]. Concomitant with the elongation of the rostral snout, the right diverticulum expands anteriorly, hence forming the snout cavity below the notochord. Finally, the left diverticulum starts fusing with the ectoderm to form the pre-oral pit, and the anlage of the mouth is clearly visible. Yet, neither one of these two structures penetrates the ectoderm and opens to the exterior at this stage [47].

The earliest larva, at the L0 stage, already features the main structural elements that define the asymmetry, along the left-right axis, of all subsequent larval stages (Fig. 4C). Thus the larval mouth opens on the left side of the developing animal by fusion of ectoderm and endoderm [47,48]. In addition, the left diverticulum has now penetrated the ectoderm to form the pre-oral pit. Although the function of the lancelet pre-oral pit is still debated [49], Hatschek's pit, as it is alternatively called, is a likely homolog of the vertebrate adenohypophysis [50]. Hatschek's nephridium, the larval lancelet kidney, is now detectable between the ectoderm and the anterior-most somite on the left side of the larva [17,48]. On the right side, the club-shaped gland is forming in the anterior endoderm, opposite to the mouth [51]. Once completely developed, the club-shaped gland resembles a tube that connects the pharyngeal lumen on the right with the external environment on the left [52]. The opening is located just anterior to the mouth and is characterized by cells bearing large cilia that create a water current from the

exterior into the organ [53]. The club-shaped gland has been shown to secrete mucoproteins and might thus contribute to larval feeding [1]. Another structure detectable on the right side of the pharynx at the L0 stage is the endostyle. The endostyle forms from a thickening of the endodermal wall and is located just anterior to the club-shaped gland. The endostyle, which secretes mucous used to trap food particles, has been proposed to be homologous to the vertebrate thyroid gland [2,54,55].

Although the definitive gill slits of the lancelet larva are located on the right side of the body, the anlage of the first gill slit forms almost at the ventral midline of the L0 larva [1]. At the same stage, the anlage of the anus arises at the posterior end of the gut, which is located just anterior to the ectodermal caudal fin [52]. Contrary to the gill slits, although the anlage of the anus also originates at the ventral midline, the definitive anus is located on the left side of the body [52]. The first definitive gill slit penetrates at the L1 stage, and, with the establishment of all the structures referred to above, the L1 larva starts feeding (Fig. 4D). Following the L1 stage, new gill slits are added sequentially, hence defining the subsequent developmental stages: L2 stage for 2 gill slits (Fig. 4E), L3 stage for 3 gill slits (Fig. 4F) and so on, until the larva enters metamorphosis. The number of gill slits required before a larva becomes competent to undergo metamorphosis varies between different lancelet species [4,56–58].

Branchiostoma lanceolatum ***developmental timing***

Previous developmental studies on lancelets regularly defined stages relative to the time passed since fertilization using a nomenclature based on hours

post fertilization (or hpf), although it is very well established that temperature directly affects the speed and potentially even the progression of animal development [29,59]. To define the impact of temperature on *B. lanceolatum* development, we reared embryos and larvae at three different temperatures (16ºC, 19ºC and 22ºC) and mapped their developmental progression by counting somite pairs. The obtained results clearly show that, despite a marked effect on the speed of development, the shapes of the growth curves, marking the progression of development, are very similar (Fig. 5, Supplementary Fig. 1, Supplementary Table 1). This indicates that the different temperatures predominantly impact the rate of cell division during development and not the overall physiology of the embryos and larvae. It is, however, almost certain that *B. lanceolatum* can only development within a certain temperature range. *B. lanceolatum* adults, for example, die after being cultured at 30ºC for two weeks, and it is likely that embryos and larvae are even more temperature sensitive than adults [29]. Making use of these growth curves and our updated staging system, stage nomenclatures based on developmental time after fertilization, even if obtained at different temperatures, can easily be transformed into an unambiguous stage name, as defined in this work.

Comparative lancelet developmental staging

We next validated that the staging table we elaborated using *B. lanceolatum* can be applied to the development of other lancelets. We thus compared *B. lanceolatum* (Fig. 6) with four additional lancelet species, three from the genus *Branchiostoma* (*B. floridae*, *B. belcheri*, *B. japonicum*) and one from the genus

Asymmetron (*A. lucayanum*) (Table 1). A total of 12 developmental stages (8-cell, 64-cell, 128-cell, B, G1, G4, G6, N1, N2, N4, T1 and L2) plus unfertilized eggs were included in the comparative analysis (Fig. 7). DIC images of the different stages revealed no major morphological differences between different lancelet species. The defining characters for each developmental stage thus seem to be conserved. However, differences were detected in the overall size of the developing lancelets. The unfertilized egg of *B. floridae*, for example, is significantly larger than those of the other analyzed species. The diameter of the *B. floridae* egg is thus 25% larger than that of *B. lanceolatum*, 18% larger than that of *B. belcheri*, 22% larger than that of *B. japonicum* and 33% larger than that of *A. lucayanum* (Fig. 7A). The cleavage, gastrula and neurula stages of the five lancelet species are remarkably similar (Fig. 7A,B), the only notable difference being the appearance of pigmentation in the posterior-most ectoderm, which is detectable as early as the N4 stage in *A. lucayanum* and thus much earlier than in the *Branchiostoma* species (Fig. 7B,C).

Morphological differences become more evident as development proceeds. For example, although the key features of the T1 stage, such as the first pigment spot and the anlagen of mouth and pre-oral pit, are still present in all five species, the timing for the formation of rostrum and tail fin does not seem to be strictly conserved (Fig. 7C). Thus, while the rostrum is clearly elongated in *B. lanceolatum*, development of the snout region is much less advanced in the other species, in particular in *A. lucayanum* (Fig. 7C). The lack of anterior head cavities in *Asymmetron* might at least partially explain this prominent difference [5,22]. Posteriorly, pigmented cells are now detectable in *A. lucayanum* as well as *B.*

lanceolatum and *B. belcheri*. In these three lancelet species, the rudiment of the forming tail fin is also already present at the T1 stage (Fig. 7C). In the larva, the species-specific differences in the snout and tail regions become even more accentuated. While *B. lanceolatum* larvae have a particularly long and thin snout, the rostrum of the other lancelet species is much less pronounced. Furthermore, the tail fins are either pigmented and pointy (as in *A. lucayanum*, *B. lanceolatum* and *B. belcheri*) or scarcely pigmented and roundish (as in *B. floridae* and *B. japonicum*).

Taken together, although there are notable species-specific differences, we found that the development of the five lancelets we analyzed here is highly conserved. It was thus very easy to apply our updated staging and stage nomenclature systems to these five species representing two of the three lancelet genera. We expect this updated developmental staging system to be universal and applicable to embryos and larvae from all extant lancelets.

Discussion

In the present study, we carried out a detailed analysis of the development of the lancelet *B. lanceolatum* using confocal microscopy and defined straightforward staging and nomenclature systems for developing lancelets. We validated this updated staging system at different rearing temperatures for *B. lanceolatum* and demonstrated that it can be used for staging lancelets from the genus *Branchiostoma* as well as from the genus *Asymmetron*. This work thus remedies a significant problem for studies carried out in lancelets: the lack of

comparability between embryos and larvae from different species. Importantly, the morphological characters used to define each stage are generally easy to identify, such as the total number of cells for the cleavage stages, the initiation of asynchronous cell division for the blastula (B) stage, the shape of the gastrula (G), the number of somite pairs in the neurula (N) and tailbud (T) stages and the formation of pharyngeal structures for the tailbud (T) and larva (L) stages. Most of these characters have previously been validated as distinguishing hallmarks of lancelet development [14–20] and are also regularly used for staging other model organisms [60,61].

The updated staging system also allowed us to clarify previously unresolved controversies about lancelet development. One example is the definition of the blastula stage. Some authors suggested that the blastula is established as soon as the blastocoel is enclosed by cells (at the 64-cell stage) [57], while others proposed that the blastula forms after the 8th round of cell divisions (after the 128-cell stage) [18]. Here, we redefined the blastula (B) stage from the initiation of asynchronous cell divisions to the initial flattening of the vegetal side (G0 stage), which is in agreement with the observations by Hirakow and Kajita [18]. Another ambiguous developmental period is the transition between the gastrula and the neurula stage, sometimes referred to as a very late gastrula [19] or very early neurula [26,62]. We redefined this important stage as N0, corresponding to an embryo with a small blastopore, which is characteristic for gastrula stages, and a flattened neural plate, marking the onset of neurulation. We further expanded the classification of neurulae to six independent N stages, while Hirakow and Kajita [20] distinguished only three and Lu and colleagues [26] four N stages. Another controversial point of

lancelet development is the definition of the larva. Some authors claimed that the larval stage starts when “tissues and cells prepare for performing their own function” [20]. Alternatively, the larval stage has been defined by the opening of the mouth and thus by the moment the animal starts feeding [1]. To clarify this issue, we defined a new developmental period for lancelets that, based on the gestalt of the embryo at this stage, we called the tailbud (T) [63]. Furthermore, we defined the onset of the larval stage (L0) as the moment when the mouth opens, as has previously been suggested in the literature [1]. Our detailed analysis of developing *B. lanceolatum* thus not only yielded an updated staging system, but also clarified several disputed issues about lancelet development.

Conclusions

The lancelets are the sister group of vertebrates and tunicates and occupy a basal position within the phylum Chordata [1,2]. This position within the tree of life explains the importance of lancelets for understanding the evolution of chordates and vertebrates. Great efforts have thus been made to develop protocols for maintaining and spawning adults in captivity and for manipulating embryos and larvae [4]. Thanks to these efforts, lancelets have become attractive laboratory models [4]. Yet, one of the remaining flaws was the absence of a universal staging system guaranteeing the comparability of results obtained in different lancelet species. Here, we propose a complete staging system for developing lancelets. Although the stage descriptions were carried out in *B. lanceolatum*, our comparisons with other lancelet species clearly demonstrate that both staging and

nomenclature are valid beyond *B. lanceolatum* and are likely applicable to all extant lancelets. In this regard, this work adds morphological evidence to the genetic results suggesting that lancelets evolve only very slowly [12,24,25,64]. Taken together, although this work is certainly not the first to attempt to classify lancelet development, we strongly believe that our description and organization of lancelet embryonic and larval development should become the standard for the scientific community in an effort to homogenize research on developing lancelets.

Methods

Animal husbandry, in vitro *cultures and fixation*

Ripe *B. lanceolatum* were collected by dredging in Argelès-sur-Mer, France, and retrieved from the sand by sieving. Adults were transported, quarantined and maintained as previously described [4]. Spawning was induced by a 36-hour thermal shock at 23ºC. Sperm and oocytes were collected separately and fertilization was performed *in vitro*. *B. lanceolatum* embryos and larvae were raised in the dark at constant temperatures (16ºC, 19ºC or 22ºC) until the desired stage, and larvae were fed as previously described [4].

Adult *B. floridae* were collected in Tampa Bay, Florida, USA. Animals were maintained in the laboratory as previously described [65,66]. Gametes were obtained either by electric stimulation, heat shock or spontaneous spawning [57,67]. To verify, whether ripe adults spawned spontaneously, a hand-held sieve was dredged through the sand one hour after the lights were turned off. Embryos and larvae were cultured at constant temperatures (25ºC or 30ºC) until the desired stage, and larvae were fed with *Isochrysis sp.* algae.

Adult *B. belcheri* and *B. japonicum* were collected in Kinmen Island near Xiamen in southeastern China [62]. Animals were maintained as previously described [65,66]. Embryos were obtained through spontaneous spawning in the facility [65]. Embryos and larvae were cultured at a constant temperature (23ºC-24ºC for *B. belcheri* and 25ºC for *B. japonicum*) until the desired stage, and larvae were fed with *Isochrysis sp.* algae.

A. lucayanum adults were collected in the lagoon between North and South Bimini, Bahamas. Embryos and larvae were obtained and subsequently cultured at a constant temperature (27ºC) as previously described [5].

Embryos and larvae used for differential interference contrast (DIC) microscopy were fixed in 4% PFA in MOPS buffer for 1 hour at room temperature or overnight at 4ºC. Embryos and larvae were subsequently washed twice in ice-cold 70% ethanol in DEPC-water and stored at -20ºC until further use. Embryos and larvae were rehydrated in PBS or PBS-Tween20 buffer and mounted in PBS buffer or 80% glycerol for imaging.

Fluorescent staining, immunohistochemistry and* in situ *hybridization

Live *B. lanceolatum* cleavage- and gastrula-stage embryos were stained using FM 4-64 lipophilic dye (Invitrogen, Cergy Pontoise, France) at a final working concentration of 10 µg/ml [68]. Following a 1-hour fixation with freshly prepared 4% paraformaldehyde in MOPS buffer at room temperature [69], the embryos were washed twice in 70% ethanol and subsequently rehydrated in PBS buffer [69]. Nuclear DNA staining was performed for 10 minutes at room temperature using Hoechst dye (Invitrogen, Cergy Pontoise, France) at a final dilution of 1:5000. Embryos were imaged within 3 hours after staining with the FM 4-64 and Hoechst dyes. No nuclear DNA staining was observable prior to the 128-cell stage, which might be related to size and lipid content of early cleavage stages.

For whole-mount immunohistochemistry and *in situ* hybridization, *B. lanceolatum* embryos and larvae were fixed overnight at 4ºC in freshly prepared ice-cold 4% paraformaldehyde in MOPS buffer [69]. Immunohistochemistry was

performed as previously described [70], using a primary antibody against aPKC (polarity protein atypical protein kinase C) (SC216, Santa Cruz Biotechnology, Dallas, USA) at final dilution of 1:100 and a secondary anti-mouse IgG-heavy and light chain antibody conjugated with Cy3™ (A90-516C3, Bethyl Laboratories Inc., Montgomery, USA) at a final dilution of 1:200. Hoechst dye (Invitrogen, Cergy Pontoise, France) at a final dilution of 1:5000 was used for nuclear DNA staining. For *in situ* hybridization, a 874-bp fragment containing the complete coding sequence of the *B. lanceolatum mrf1* (myogenic regulatory factor 1) gene (GenBank accession number MT452570) was amplified by PCR from cDNA and cloned in the pGEM-T Easy Vector. The *in situ* hybridization experiments were subsequently carried out with a *mrf1*-specific antisense riboprobe as previously described [69,71].

Image acquisition and processing

Confocal imaging was carried out on a Leica TCS SP8 confocal microscope, using a 20x objective (0.75 IMM HC PL APO CORR CS WD = 0,68mm) (Leica Microsystems SAS, Nanterre, France). Series of optical sections were taken at a z-step interval of 2 µm. The ImageJ software [72] was subsequently used for image processing and to generate maximum as well as average projections. Adobe Photoshop CS6 (Adobe Inc., San Jose, USA) was used to process larger images (larval stages) requiring the reconstitution from partial pictures.

DIC microscopy of *B. lanceolatum* embryos and larvae was performed using a Zeiss Axiophot microscope equipped with an AxioCam ERc 5s camera (Carl Zeiss SAS, Marly-le-Roi, France). Images of *B. floridae*, *B. belcheri*, *B. japonicum*

and *A. lucayanum* embryos and larvae were acquired with a Zeiss Axio Imager A1 microscope (Carl Zeiss SAS, Marly-le-Roi, France). For 64-cell, 128-cell and blastula stages, multiple z-levels were taken manually. The z-stack images were processed with the Extended-Depth-of-Field plugin of the ImageJ software using default settings [72] and subsequently processed with Adobe Photoshop CS6 (Adobe Inc., San Jose, USA).

Growth curves

B. lanceolatum neurula, tailbud and larva stages were reared at three different temperatures: 16ºC, 19ºC and 22ºC. At regular intervals, animals were collected and fixed for subsequent *in situ* hybridization analyses. An antisense riboprobe targeting the *B. lanceolatum mrf1* gene, a member of the *myoD* gene family [73], was used to visualize the somites, hence allowing somite pair counts in embryos and larvae reared at different temperatures. The somite pair counts were used to define a training set of data points for each rearing temperature, hence allowing the calculation of best natural logarithmic tendency curves using Microsoft Excel (Microsoft Corporation, Redmond, USA). The curves were subsequently curated to define time periods for each developmental stage.

Acknowledgements

The authors are indebted to Linda Z. Holland and Nicholas D. Holland from the Scripps Institution of Oceanography, La Jolla, USA, for collecting *Asymmetron lucayanum* adults. Janet Chenevert from the Laboratoire de Biologie du Développement de Villefranche-sur-Mer, Villefranche-sur-Mer, France, kindly provided the FM 4-64 lipophilic dye and the primary antibody against aPKC as well as useful technical advice. We would like to thank the Centre de Ressources Biologiques (CRB) of the Institut de la Mer de Villefranche (IMEV), specifically the Service Aquariologie (SA) and the Mediterranean Culture Collection of Villefranche (MCCV), both of which are financed by EMBRC-France (ANR-10-INBS-02), and the Plateforme d'Imagerie par Microscopie (PIM) of the Institut de la Mer de Villefranche (IMEV). João E. Carvalho was a FCT doctoral fellow (SFRH/BD/86878/2012) and is currently supported by a FRM fellowship (SPF20170938703).

References

1. Holland LZ. Cephalochordata. In: Wanninger A, editor. Evol Dev Biol Invertebr. Springer; 2015. p. 91–133.
2. Bertrand S, Escriva H. Evolutionary crossroads in developmental biology: amphioxus. Development. 2011;138:4819–30.
3. Louis A, Crollius HR, Robinson-Rechavi M. How much does the amphioxus genome represent the ancestor of chordates? Brief Funct Genomics. 2012;11:89–95.
4. Carvalho JE, Lahaye F, Schubert M. Keeping amphioxus in the laboratory: an update on available husbandry methods. Int J Dev Biol. 2017;61:773–83.
5. Holland ND, Holland LZ. Laboratory spawning and development of the Bahama lancelet, *Asymmetron lucayanum* (cephalochordata): fertilization through feeding larvae. Biol Bull. 2010;219:132–41.
6. Kon T, Nohara M, Yamanoue Y, Fujiwara Y, Nishida M, Nishikawa T. Phylogenetic position of a whale-fall lancelet (cephalochordata) inferred from whole mitochondrial genome sequences. BMC Evol Biol. 2007;7:127.
7. Nishikawa T. A new deep-water lancelet (Cephalochordata) from off Cape Nomamisaki, SW Japan, with a proposal of the revised system recovering the genus *Asymmetron*. Zoolog Sci. 2004;21:1131–6.
8. Poss SG, Boschung HT. Lancelets (cephalochordata: Branchiostomatidae): how many species are valid? Isr J Zool. 1996;42:S13–66.
9. Yue J-X, Yu J-K, Putnam NH, Holland LZ. The transcriptome of an amphioxus, *Asymmetron lucayanum*, from the Bahamas: a window into chordate evolution. Genome Biol Evol. 2014;6:2681–96.
10. Zhang Q-J, Zhong J, Fang S-H, Wang Y-Q. *Branchiostoma japonicum* and *B. belcheri* are distinct lancelets (Cephalochordata) in Xiamen waters in China. Zoolog Sci. 2006;23:573–9.
11. Subirana L, Farstey V, Bertrand S, Escriva H. *Asymmetron lucayanum*: how many species are valid? PLOS ONE. 2020;15:e0229119.

12. Igawa T, Nozawa M, Suzuki DG, Reimer JD, Morov AR, Wang Y, et al. Evolutionary history of the extant amphioxus lineage with shallow-branching diversification. Sci Rep. 2017;7:1157.
13. Holland ND, Holland LZ. The ups and downs of amphioxus biology: a history. Int J Dev Biol. 2017;61:575–83.
14. Kovalevsky AO. Entwicklungsgeschichte des *Amphioxus lanceolatus*. Mém Académie Impérial Sci St Pétersbourg. 1867;XI.
15. Cerfontaine P. Recherches sur le développement de l'Amphioxus. Impr. H. Vaillant-Carmanne; 1906.
16. Conklin EG. The embryology of amphioxus. J Morphol. 1932;54:69–151.
17. Hatschek B. The Amphioxus and its development. Tuckey J, editor. London: Swan Sonnenschein & Co.; 1893
18. Hirakow R, Kajita N. An electron microscopic study of the development of amphioxus, *Branchiostoma belcheri tsingtauense*: Cleavage. J Morphol. 1990;203:331–44.
19. Hirakow R, Kajita N. Electron microscopic study of the development of amphioxus, *Branchiostoma belcheri tsingtauense*: The gastrula. J Morphol. 1991;207:37–52.
20. Hirakow R, Kajita N. Electron microscopic study of the development of amphioxus, *Branchiostoma belcheri tsingtauense*: the neurula and larva. Kaibogaku Zasshi. 1994;69:1–13.
21. Stokes MD, Holland ND. Embryos and larvae of a lancelet, *Branchiostoma floridae*, from hatching through metamorphosis: growth in the laboratory and external morphology. Acta Zool. 1995;76:105–20.
22. Holland ND, Holland LZ, Heimberg A. Hybrids between the Florida amphioxus (*Branchiostoma floridae*) and the Bahamas lancelet (*Asymmetron lucayanum*): developmental morphology and chromosome counts. Biol Bull. 2015;228:13–24.
23. Acemel RD, Tena JJ, Irastorza-Azcarate I, Marlétaz F, Gómez-Marín C, de la Calle-Mustienes E, et al. A single three-dimensional chromatin compartment in amphioxus indicates a stepwise evolution of vertebrate Hox bimodal regulation. Nat Genet. 2016;48:336–41.

24. Marlétaz F, Firbas PN, Maeso I, Tena JJ, Bogdanovic O, Perry M, et al. Amphioxus functional genomics and the origins of vertebrate gene regulation. Nature. 2018;564:64–70.

25. Simakov O, Marlétaz F, Yue J-X, O'Connell B, Jenkins J, Brandt A, et al. Deeply conserved synteny resolves early events in vertebrate evolution. Nat Ecol Evol. 2020;1–11.

26. Lu T-M, Luo Y-J, Yu J-K. BMP and Delta/Notch signaling control the development of amphioxus epidermal sensory neurons: insights into the evolution of the peripheral sensory system. Development. 2012;139:2020–30.

27. Annona G, Caccavale F, Pascual-Anaya J, Kuratani S, De Luca P, Palumbo A, et al. Nitric Oxide regulates mouth development in amphioxus. Sci Rep. 2017;7:8432.

28. Bertrand S, Camasses A, Somorjai I, Belgacem MR, Chabrol O, Escande M-L, et al. Amphioxus FGF signaling predicts the acquisition of vertebrate morphological traits. Proc Natl Acad Sci. 2011;108:9160–5.

29. Fuentes M, Benito E, Bertrand S, Paris M, Mignardot A, Godoy L, et al. Insights into spawning behavior and development of the European amphioxus (*Branchiostoma lanceolatum*). J Exp Zoolog B Mol Dev Evol. 2007;308B:484–493.

30. Pantzartzi CN, Pergner J, Kozmikova I, Kozmik Z. The opsin repertoire of the European lancelet: a window into light detection in a basal chordate. Int J Dev Biol. 2017;61:763–72.

31. Holland LZ, Onai T. Early development of cephalochordates (amphioxus). WIREs Dev Biol. 2012;1:167–83.

32. Holland LZ, Holland ND. Early development in the lancelet (= Amphioxus) *Branchiostoma floridae* from sperm entry through pronuclear fusion - presence of vegetal pole plasm and lack of conspicuous ooplasmic segregation. Biol Bull. 1992;182:77–96.

33. Willey A. Amphioxus and the ancestry of the vertebrates. London: Macmillan and Co.; 1894.

34. Wu H-R, Chen Y-T, Su Y-H, Luo Y-J, Holland LZ, Yu J-K. Asymmetric localization of germline markers *Vasa* and *Nanos* during early development in the amphioxus *Branchiostoma floridae*. Dev Biol. 2011;353:147–59.

35. Holland ND, Holland LZ. Fine structural study of the cortical reaction and formation of the egg coats in a lancelet (= amphioxus), *Branchiostoma floridae* (phylum Chordata: subphylum Cephalochordata = Acrania). Biol Bull. 1989;176:111–22.

36. Grassé P-P. Traité de zoologie: anatomie, systématique, biologie - Tome XI, Echinodermes - Stomocordes - Procordes. Paris: Masson & Cie; 1948.

37. Tung TC, Wu SC, Tung YYF. Experimental studies on neural induction in Amphioxus. Sci Sin. 1961;7:263–70.

38. Tung TC, Wu SC, Tung YYF. The presumptive areas of the egg of amphioxus. Sci Sin. 1962;11:629–644.

39. Yu J-K, Satou Y, Holland ND, Shin-I T, Kohara Y, Satoh N, et al. Axial patterning in cephalochordates and the evolution of the organizer. Nature. 2007;445:613–7.

40. Onai T, Yu J-K, Blitz IL, Cho KWY, Holland LZ. Opposing Nodal/Vg1 and BMP signals mediate axial patterning in embryos of the basal chordate amphioxus. Dev Biol. 2010;344:377–89.

41. Hatschek B. Studien über entwicklung des Amphioxus. Wien: A. Hölder; 1881.

42. Stokes M. Larval locomotion of the lancelet. J Exp Biol. 1997;200:1661–80.

43. Kozmik Z, Holland ND, Kalousova A, Paces J, Schubert M, Holland LZ. Characterization of an amphioxus paired box gene, *AmphiPax2/5/8*: developmental expression patterns in optic support cells, nephridium, thyroid-like structures and pharyngeal gill slits, but not in the midbrain-hindbrain boundary region. Development. 1999;126:1295–304.

44. Kozmik Z, Holland ND, Kreslova J, Oliveri D, Schubert M, Jonasova K, et al. *Pax–Six–Eya–Dach* network during amphioxus development: conservation in vitro but context specificity in vivo. Dev Biol. 2007;306:143–59.

45. Carvalho JE, Lahaye F, Croce JC, Schubert M. CYP26 function is required for the tissue-specific modulation of retinoic acid signaling during amphioxus development. Int J Dev Biol. 2017;61:733–47.

46. Holland ND, Holland LZ. Stage- and tissue-specific patterns of cell division in embryonic and larval tissues of amphioxus during normal development. Evol Dev. 2006;8:142–9.

47. Kaji T, Reimer JD, Morov AR, Kuratani S, Yasui K. Amphioxus mouth after dorso-ventral inversion. Zool Lett. 2016;2.

48. Holland ND. Formation of the initial kidney and mouth opening in larval amphioxus studied with serial blockface scanning electron microscopy (SBSEM). EvoDevo. 2018;9:16.

49. Candiani S, Holland ND, Oliveri D, Parodi M, Pestarino M. Expression of the amphioxus Pit-1 gene (*AmphiPOU1F1/Pit-1*) exclusively in the developing preoral organ, a putative homolog of the vertebrate adenohypophysis. Brain Res Bull. 2008;75:324–30.

50. Stach T. On the preoral pit of the larval amphioxus (*Branchiostoma lanceolatum*). Ann Sci Nat Zool Biol Anim. 1996;17:129–134.

51. Goodrich ES. Memoirs: The development of the club-shaped gland in amphioxus. J Cell Sci. 1930;s2-74:155–64.

52. Jefferies RPS. The ancestry of the vertebrates. Cambridge: Cambridge University Press; 1987.

53. Olsson R. Club-shaped gland and endostyle in larval *Branchiostoma lanceolatum* (Cephalochordata). Zoomorphology. 1983;103:1–13.

54. Paris M, Escriva H, Schubert M, Brunet F, Brtko J, Ciesielski F, et al. Amphioxus postembryonic development reveals the homology of Chordate metamorphosis. Curr Biol. 2008;18:825–30.

55. Ogasawara M. Overlapping expression of amphioxus homologs of the thyroid transcription factor-1 gene and thyroid peroxidase gene in the endostyle: insight into evolution of the thyroid gland. Dev Genes Evol. 2000;210:231–42.

56. Urata M, Yamaguchi N, Henmi Y, Yasui K. Larval development of the Oriental lancelet, *Branchiostoma belcheri*, in laboratory mass culture. Zoolog Sci. 2007;24:787–97.

57. Holland LZ, Yu J-K. Cephalochordate (amphioxus) embryos: procurement, culture, and basic methods. Methods Cell Biol. 2004;74:195–215.

58. Wickstead JH. *Branchiostoma lanceolatum* larvae: some experiments on the effect of thiouracil on metamorphosis. J Mar Biol Assoc U K. 1967;47:49–59.

59. Ebisuya M, Briscoe J. What does time mean in development? Development. 2018;145:dev164368.

60. Kimmel CB, Ballard WW, Kimmel SR, Ullmann B, Schilling TF. Stages of embryonic development of the zebrafish. Dev Dyn. 1995;203:253–310.

61. Richardson MK, Wright GM. Developmental transformations in a normal series of embryos of the sea lamprey *Petromyzon marinus* (linnaeus). J Morphol. 2003;257:348–63.

62. Zhang Q-J, Luo Y-J, Wu H-R, Chen Y-T, Yu J-K. Expression of germline markers in three species of amphioxus supports a preformation mechanism of germ cell development in cephalochordates. EvoDevo. 2013;4:17.

63. Lemaire P. Evolutionary crossroads in developmental biology: the tunicates. Development. 2011;138:2143–52.

64. Putnam NH, Butts T, Ferrier DEK, Furlong RF, Hellsten U, Kawashima T, et al. The amphioxus genome and the evolution of the chordate karyotype. Nature. 2008;453:1064–71.

65. Zhang Q-J, Sun Y, Zhong J, Li G, Lü X-M, Wang Y-Q. Continuous culture of two lancelets and production of the second filial generations in the laboratory. J Exp Zoolog B Mol Dev Evol. 2007;308B:464–72.

66. Yong LW, Kozmikova I, Yu J-K. Using amphioxus as a basal chordate model to study BMP signaling pathway. In: Rogers MB, editor. Bone Morphog Proteins Methods Protoc. New York, NY: Springer; 2019. p. 91–114.

67. Ono H, Koop D, Holland LZ. Nodal and Hedgehog synergize in gill slit formation during development of the cephalochordate *Branchiostoma floridae*. Development. 2018;145:dev162586.

68. Sardet C, McDougall A, Yasuo H, Chenevert J, Pruliere G, Dumollard R, et al. Embryological methods in ascidians: the Villefranche-sur-Mer protocols. Vertebr Embryogenesis. 2011. p. 365–400.

69. Yu J-K, Holland LZ. Amphioxus whole-mount in situ hybridization. Cold Spring Harb Protoc. 2009;2009:pdb.prot5286.

70. Zieger E, Garbarino G, Robert NSM, Yu J-K, Croce JC, Candiani S, et al. Retinoic acid signaling and neurogenic niche regulation in the developing peripheral nervous system of the cephalochordate amphioxus. Cell Mol Life Sci. 2018;1–23.
71. Carvalho JE, Theodosiou M, Chen J, Chevret P, Alvarez S, De Lera AR, et al. Lineage-specific duplication of amphioxus retinoic acid degrading enzymes (CYP26) resulted in sub-functionalization of patterning and homeostatic roles. BMC Evol Biol. 2017;17:24.
72. Schneider CA, Rasband WS, Eliceiri KW. NIH Image to ImageJ: 25 years of image analysis. Nat Methods. 2012;9:671–5.
73. Schubert M, Meulemans D, Bronner-Fraser M, Holland LZ, Holland ND. Differential mesodermal expression of two amphioxus *MyoD* family members (*AmphiMRF1* and *AmphiMRF2*). Gene Expr Patterns. 2003;3:199–202.
74. Holland LZ, Holland ND. Developmental gene expression in amphioxus: new insights into the evolutionary origin of vertebrate brain regions, neural crest, and rostrocaudal segmentation. Am Zool. 1998;38:647–58.
75. Zhang Q-J. Taxonomy of genus *Branchiostoma* in Xiamen waters and continuous breeding of two lancelets in the laboratory [Ph.D. thesis]. [Xiamen, China]: Xiamen University; 2017.
76. Morov AR, Ukizintambara T, Sabirov RM, Yasui K. Acquisition of the dorsal structures in chordate amphioxus. Open Biol. 2016;6:160062.

Figure captions

Figure 1 – *Branchiostoma lanceolatum* cleavage and blastula stages stained with the lipophilic dye FM 4-64 (magenta). Maximum projections of confocal scans of *B. lanceolatum* embryos at the (A) 1 cell-stage, (B) 2-cell stage, (C) 4-cell stage, (D) 8-cell stage, (E) 16-cell stage, (F) 32-cell stage, (G) 64-cell stage, (H) 128-cell stage and (I) blastula stage. Insets in (D) and (E) show slender filapodia between blastomeres. Hoechst DNA staining (cyan) shows synchronous cell divisions at the 128-cell stage (H) and asynchronous cell divisions at the forming blastula B-stage (I), with highlighted in white a cell in telophase and in green a cell following cytokinesis. Abbreviations: m – maternal DNA; p – paternal DNA. Scale bar: 50 µm.

Figure 2 – *Branchiostoma lanceolatum* gastrulation stages stained with the lipophilic dye FM 4-64 (magenta) and for DNA with Hoechst (cyan). Animal pole and anterior to the left and dorsal side up. (A,B,C,D,E,F,G) Maximum projections of confocal z-stacks of the entire embryo (B',C',D',E',F',G'). Single z-stacks highlighting the inner morphology of the developing gastrula. (A) G0 stage, (B,B') G1 stage, (C,C') G2 stage, (D,D') G3 stage, (E,E') G4 stage, (F,F') G5 stage, (G,G') G6 stage. Yellow arrowhead indicates the vegetal cells (A), yellow arrow highlights the flatten side of the gastrula embryo (F), and yellow lines delimits the blastopore upper and lower lips with the embryo mid-line shown in dashed line (G').Scale bar: 50 µm.

Figure 3 – *Branchiostoma lanceolatum* neurula stages labeled for aPKC (magenta) and stained for DNA with Hoechst (cyan). Anterior pole to the left and dorsal side up. (A,B,C,D,E,F,G) Average projections of confocal z-stacks of the entire embryo (magenta) and maximum projections for Hoechst DNA staining (cyan). (B',C',D',E',F',G') Single z-stacks highlighting the inner morphology of the developing neurula. (A) N0 stage, (B,B') N1 stage, (C,C') N2 stage, (D,D') N3 stage, (E,E') N4 stage, (F,F') N5 stage. Yellow arrowheads indicate the posterior limit of the somites, and green arrowheads highlight newly establishing (C', D') or newly budding (E',F') somites. Scale bar: 100 µm.

Figure 4 – *Branchiostoma lanceolatum* tailbud and larval stages labeled for aPKC (magenta) and stained for DNA with Hoechst (cyan). Average projections of confocal z-stacks of the entire embryo (magenta) and maximum projections for Hoechst DNA staining (cyan). Anterior pole to the left and dorsal side up. (A,A') T0 stage, (B,B') T1 stage, (C) L0 stage, (D) L1 stage, (E) L2 stage, (F) L3 stage. (A',B') Single z-stacks indicating the somite number. Insets in (A,B,C,D,E,F) highlight the pharynx region. Yellow arrowheads indicate the posterior limit of the somites. Abbreviations: gs1 – 1st gill slit; gs2 – 2nd gill slit; gs3 – 3rd gill slit; m – mouth; ma – mouth anlagen. Scale bar: 100 µm.

Figure 5 – Growth curve of *Branchiostoma lanceolatum* embryos and larvae at 16ºC, 19ºC and 22ºC. Animal schematics and stage nomenclature are according to the staging system detailed in Figure 6. Tendency adjusted curves were obtained

from the training sets and are defined by the equations: [y=11.25ln(x) - 24.354] for 22ºC; [y=12.466ln(x) - 30.812] for 19ºC; and [y=12.403ln(x) - 36.493] for 16ºC. These curves use natural logarithms, thus do not reach the point 0 (0hpf) and so this part of the graph was simplified accordingly. Abbreviations: hpf – hours post fertilization.

Figure 6 – Schematic representation of lancelet development from the 1-cell stage to the L0 stage. Animal pole and anterior to the left. Drawings adapted from Hatscheck's original descriptions of *Branchiostoma lanceolatum* development [41].

Figure 7 – Comparison of lancelet development. Five species were analyzed: *Branchiostoma lanceolatum*, *Branchiostoma floridae*, *Branchiostoma belcheri*, *Branchiostoma japonicum* and *Asymmetron lucayanum*. (A) cleavage, blastula and gastrula stages, (B) neurula stages, (C) tailbud and larva stages. Cladograms represent the evolutionary relationship between the different species [12]. The green lines in (B) trace the somites on one side of the neurula, with dashed green highlighting forming somites. The green ovals in (C) indicate the gill slits of the larva. Scale bars: 100 µm.

Table 1 – Comparison of lancelet development. Species: *Branchiostoma lanceolatum*, *Branchiostoma floridae*, *Branchiostoma belcheri*, *Branchiostoma japonicum*, *Asymmetron lucayanum*. Data origin: [1] Current study, [2] [21,22,57,74], [3] [75], [4] [18–20,76], [5] [5,22]. "*" indicates data points derived from cultures obtained

by spontaneous spawning and "/" indicates that different developmental times have been reported.

Supplementary Figure 1 – Expression of the *mrf1* gene in developing *Branchiostoma lanceolatum* reared at different temperatures. Dorsal views with anterior pole to the left and right side up (A) 16ºC, (B) 19ºC and (C) 21ºC. On each image, the time of development in hours after fertilization (h) and the number of fully formed somite pairs (s) are indicated. Scale bars: 50 µm.

Supplementary Table 1 – Somite pair counts based on the expression of the *mrf1* gene in developing *Branchiostoma lanceolatum* reared at three different temperatures (Supplementary Fig. 1), and natural logarithmic tendency curves obtained from the three training sets.

Figure 1

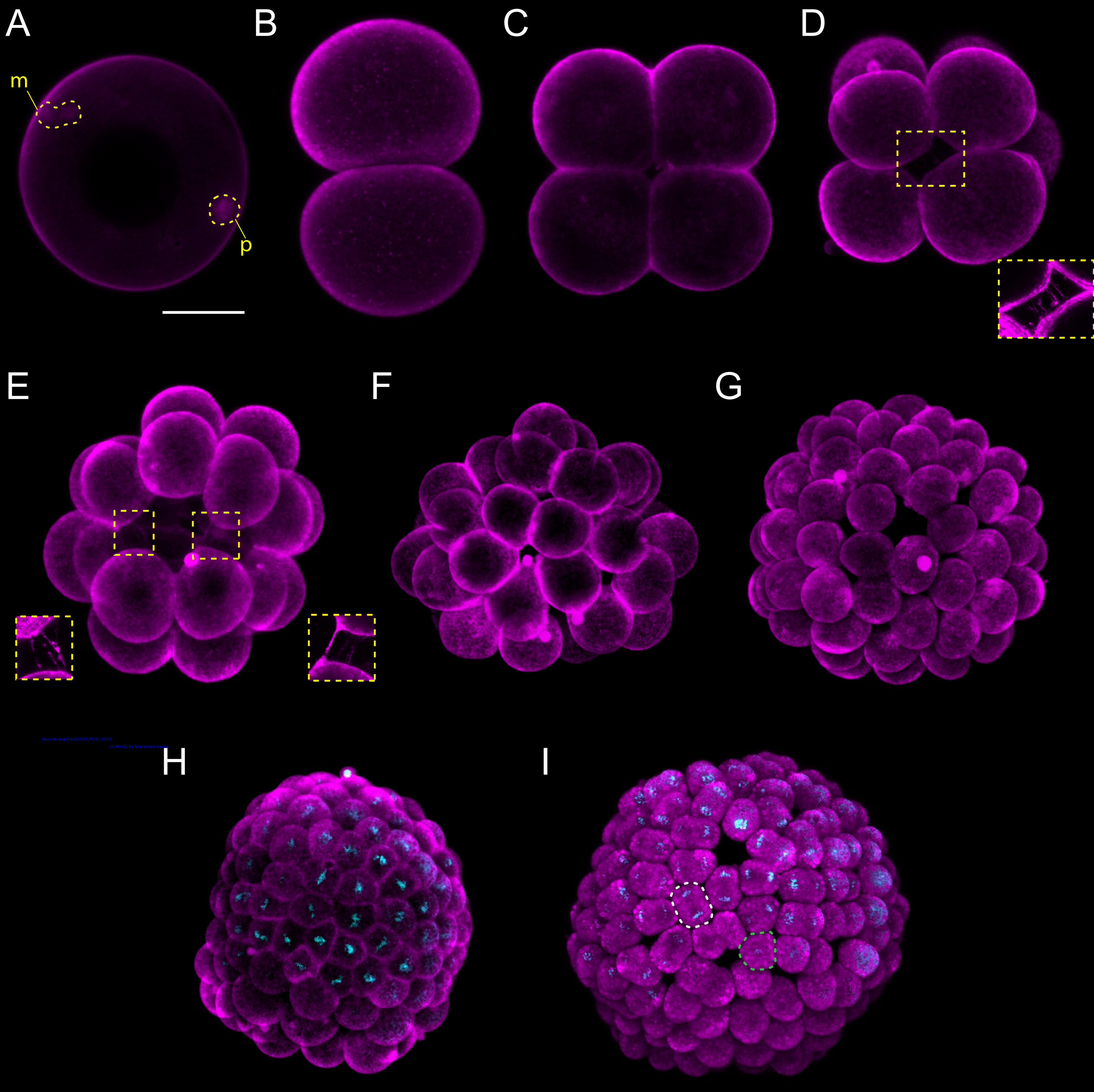

Figure 2

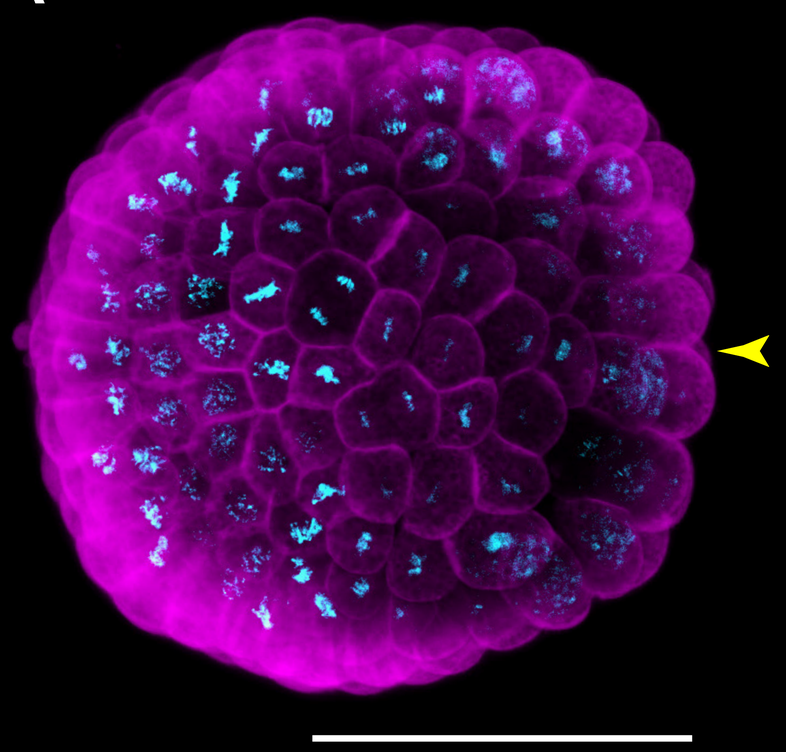

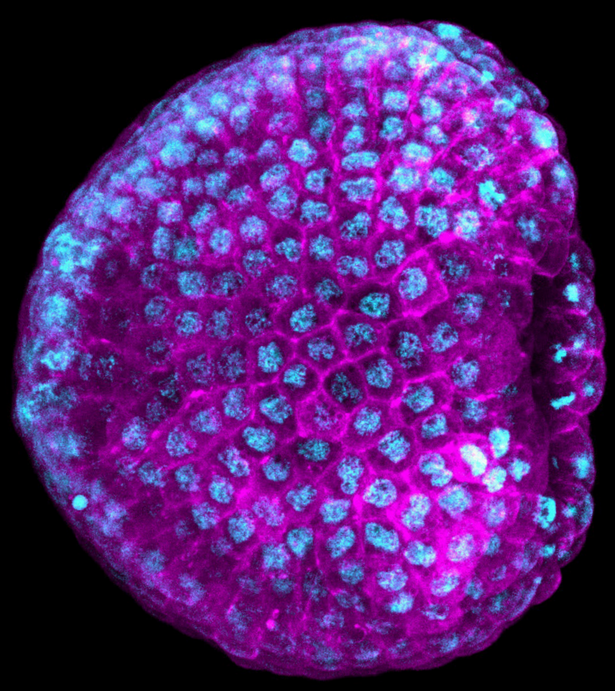

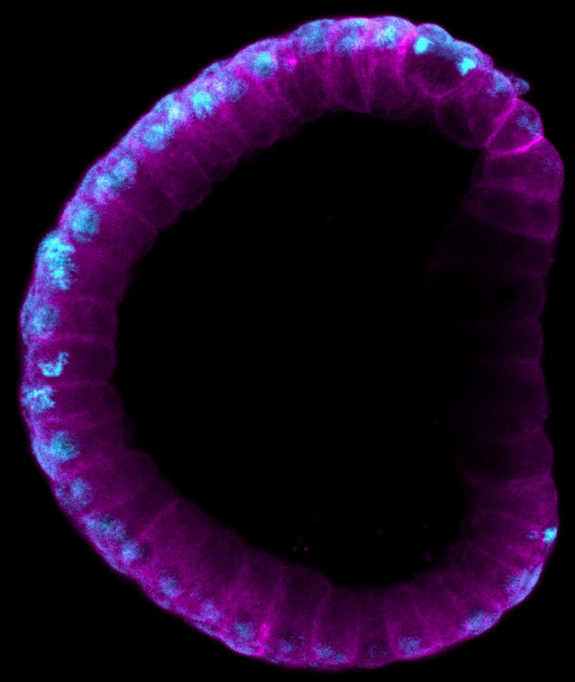

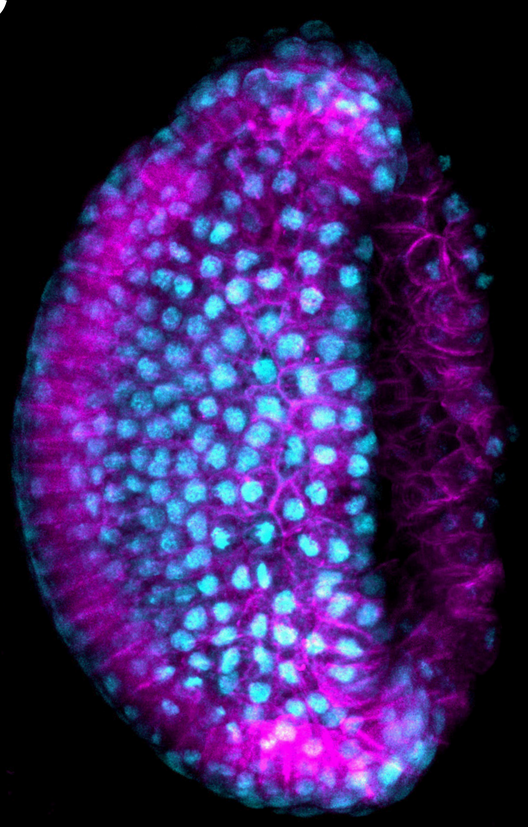

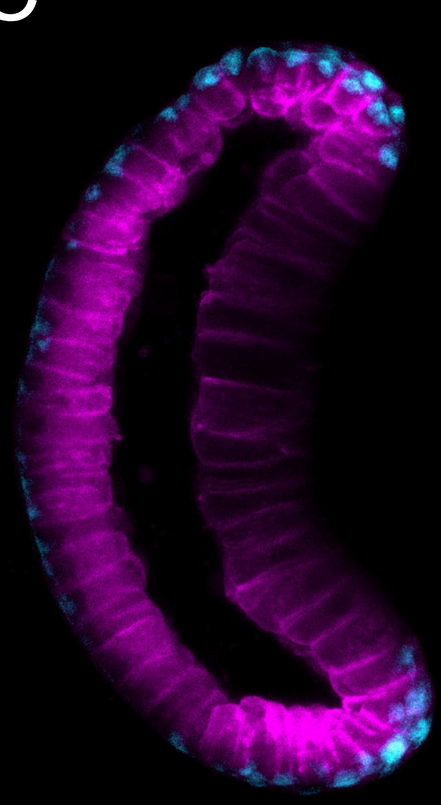

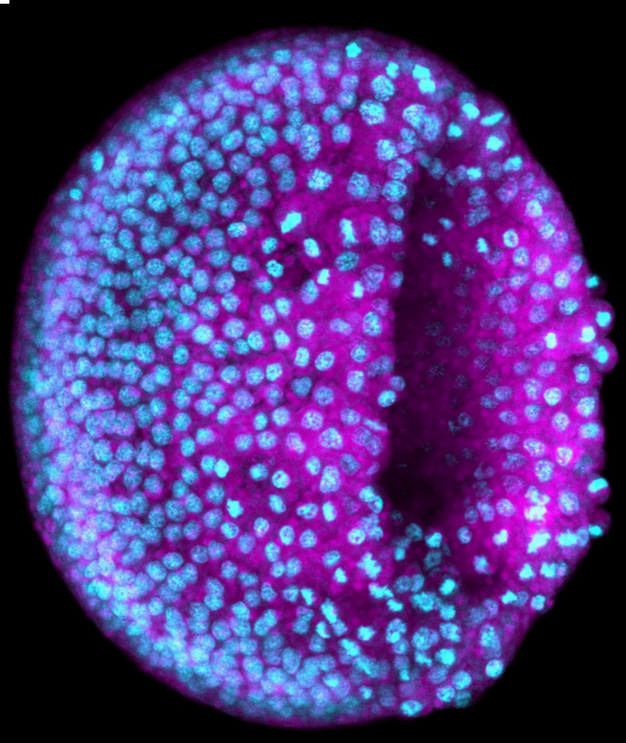

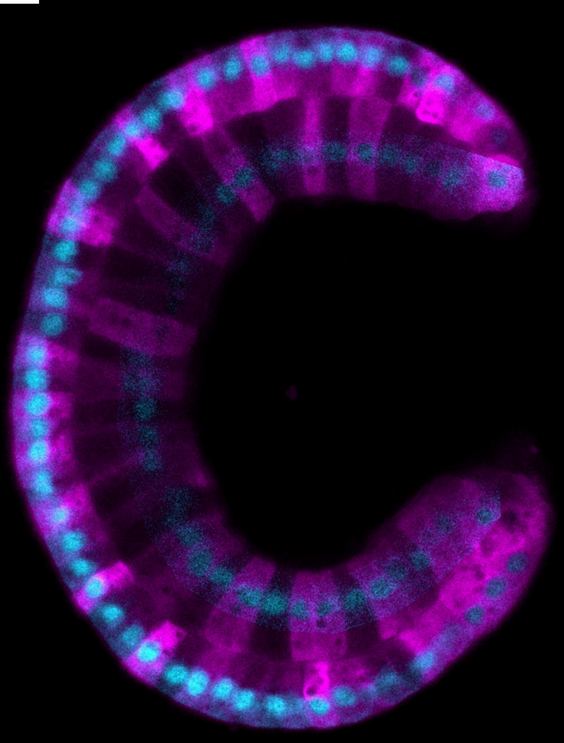

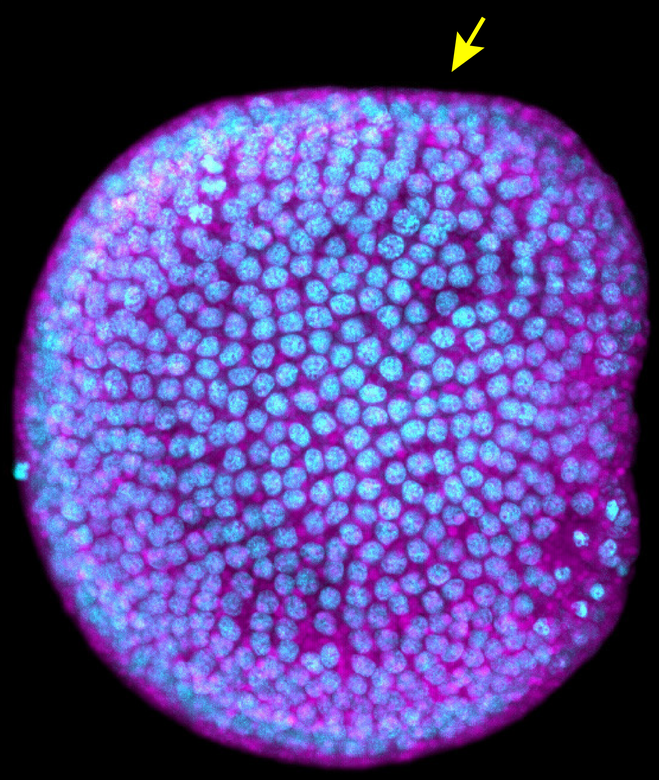

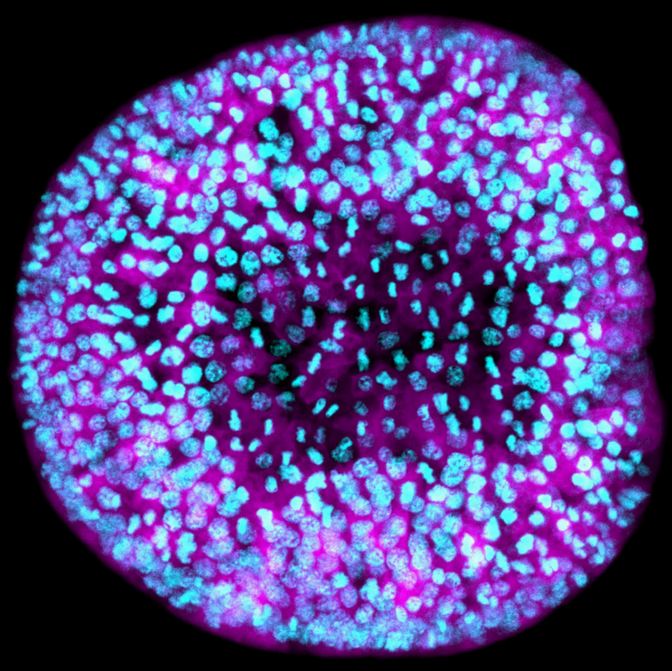

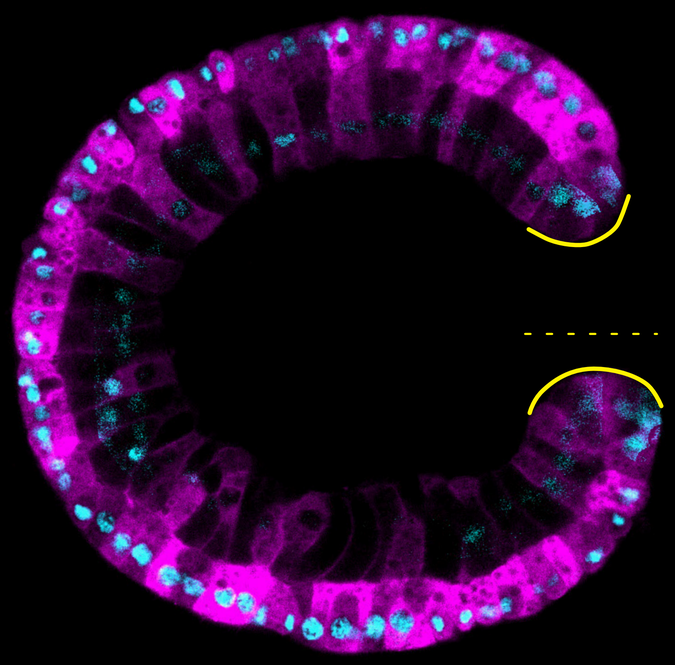

Figure 3

A

B

B’

C

C’

D

D’

E

E’

F

F’

Figure 4

A

A’

B

ma

B’

C

m

D

gs1

E

gs1 gs2

F

gs1 gs2 gs3

Figure 5

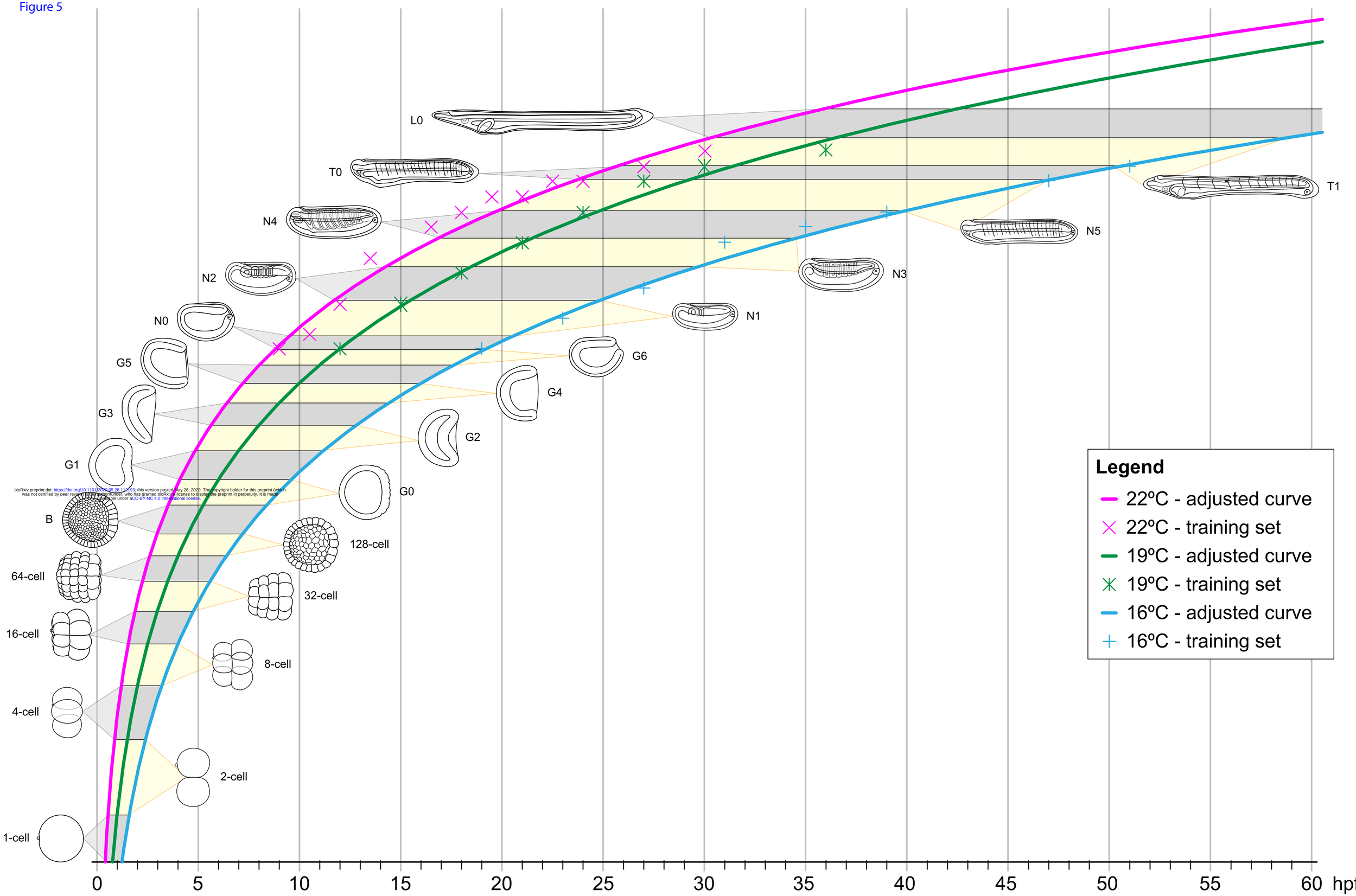

Figure 6

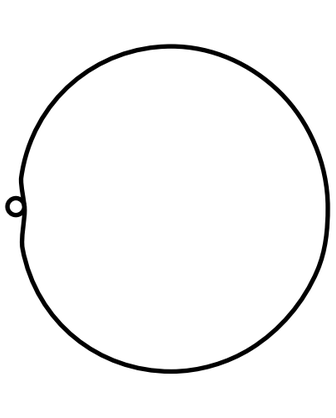

1-cell stage

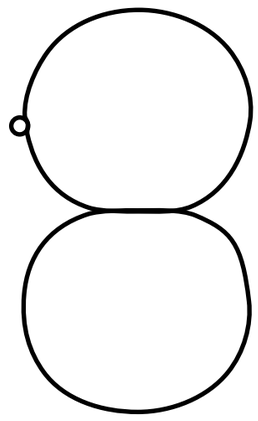

2-cell stage

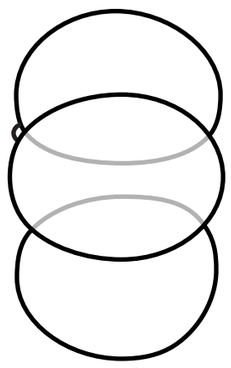

4-cell stage

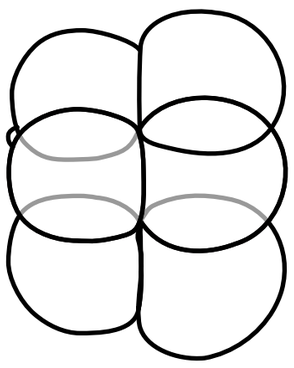

8-cell stage

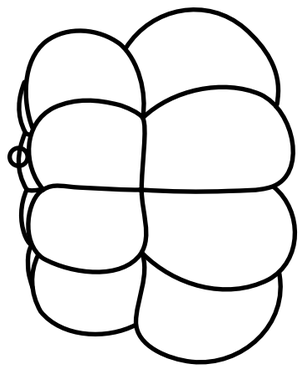

16-cell stage

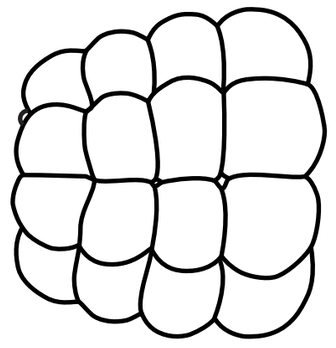

32-cell stage

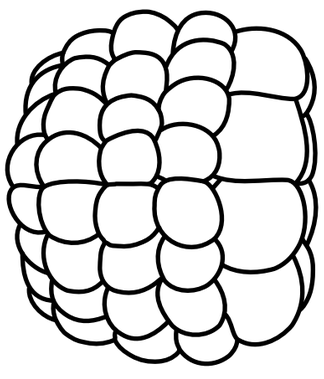

64-cell stage

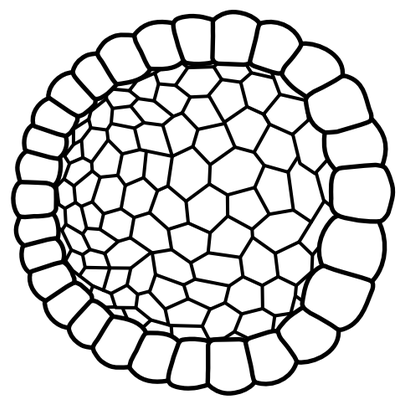

128-cell stage

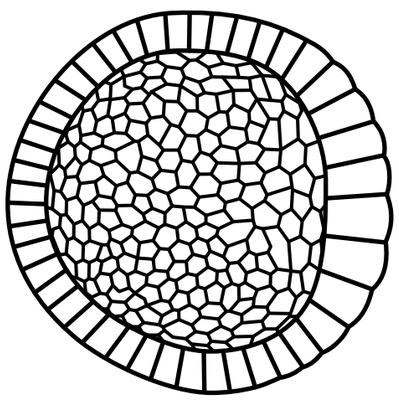

B stage

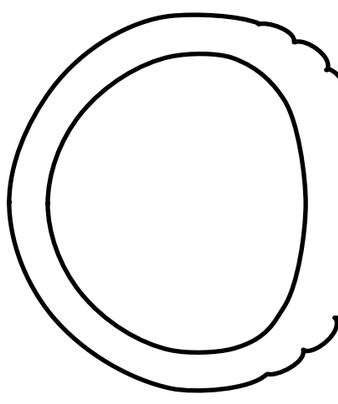

G0 stage

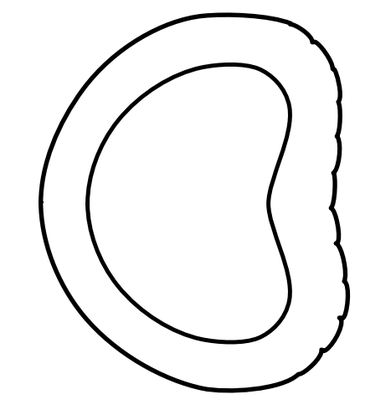

G1 stage

G2 stage

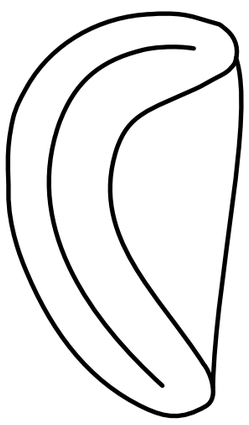

G3 stage

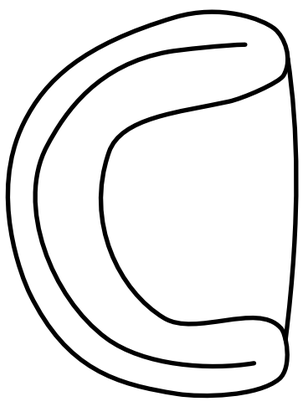

G4 stage

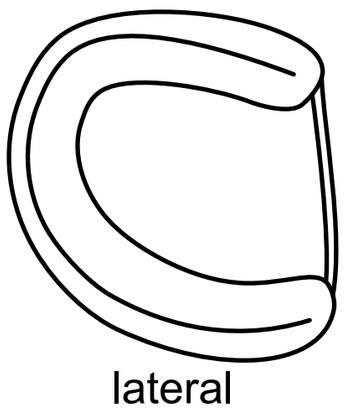

lateral

dorsal

G5 stage

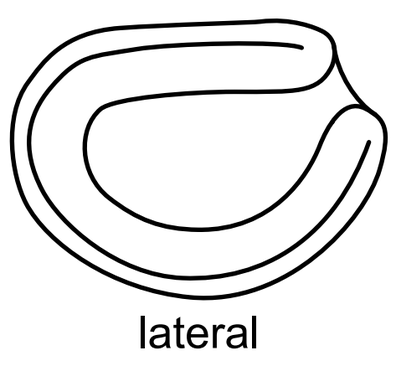

lateral

dorsal

G6 stage

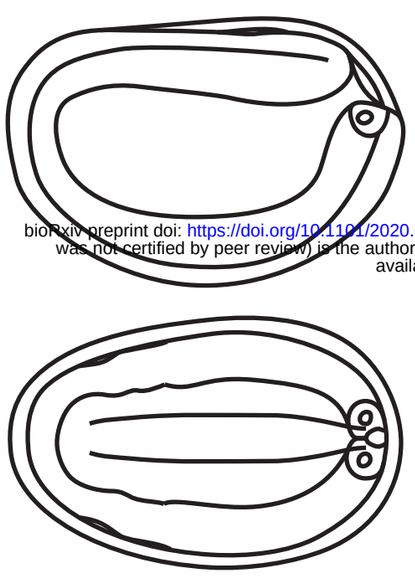

lateral

dorsal

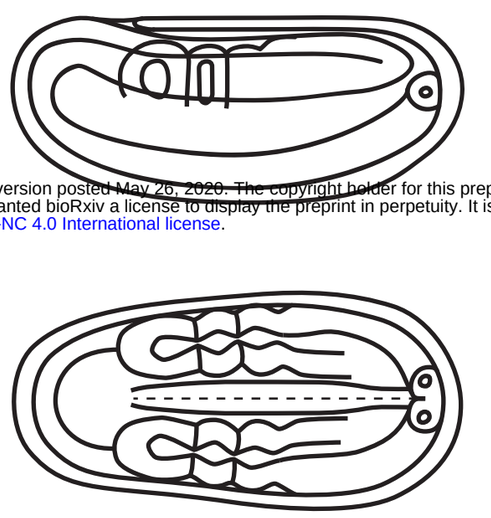

N0 stage

N1 stage

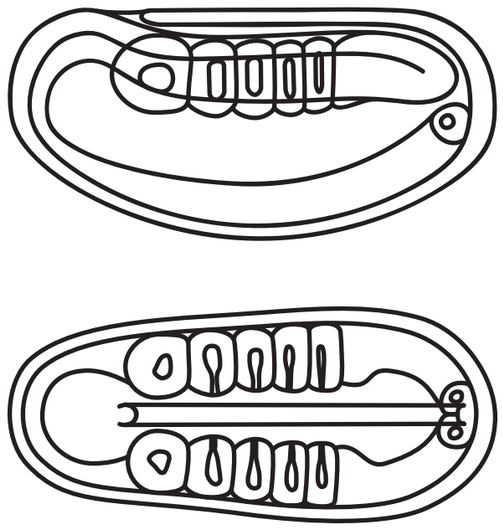

N2 stage

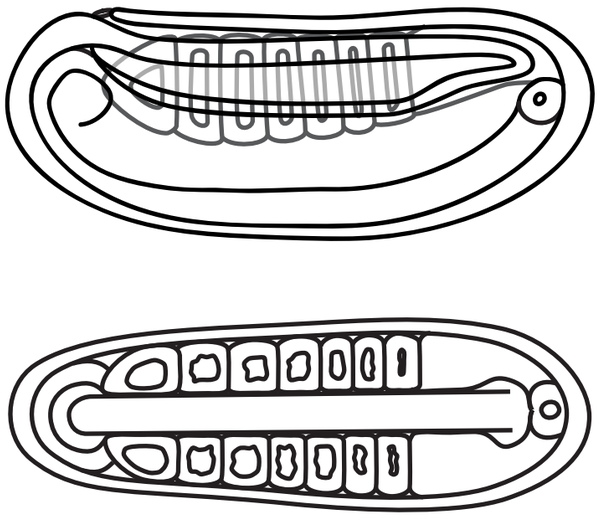

N3 stage

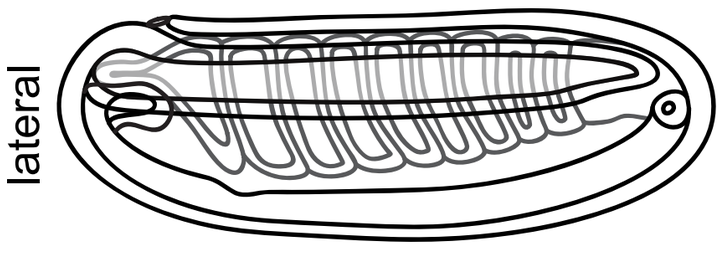

lateral

dorsal

N4 stage

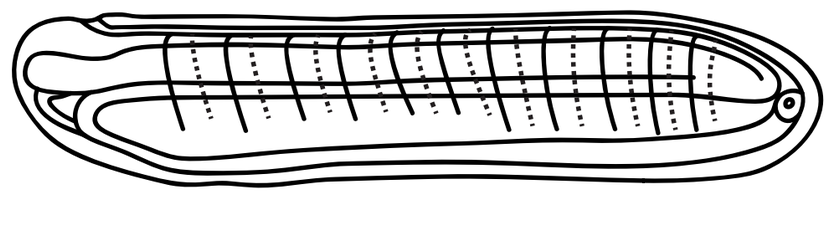

N5 stage

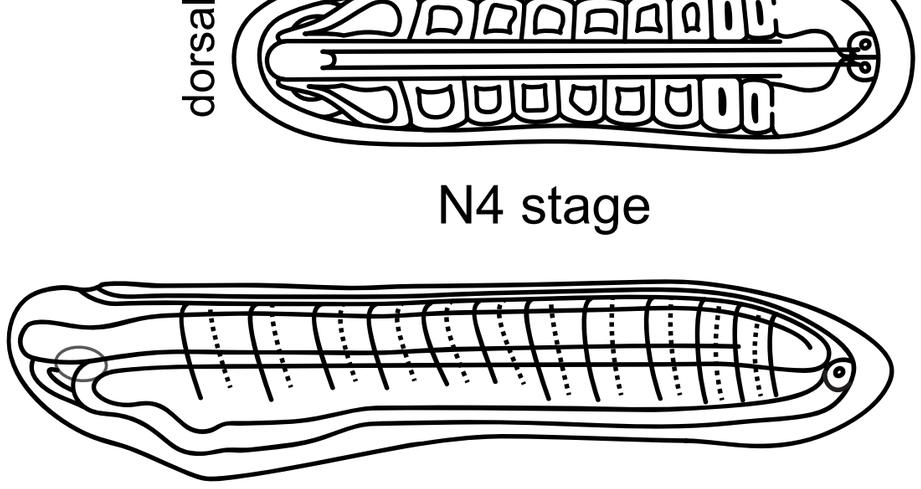

T0 stage

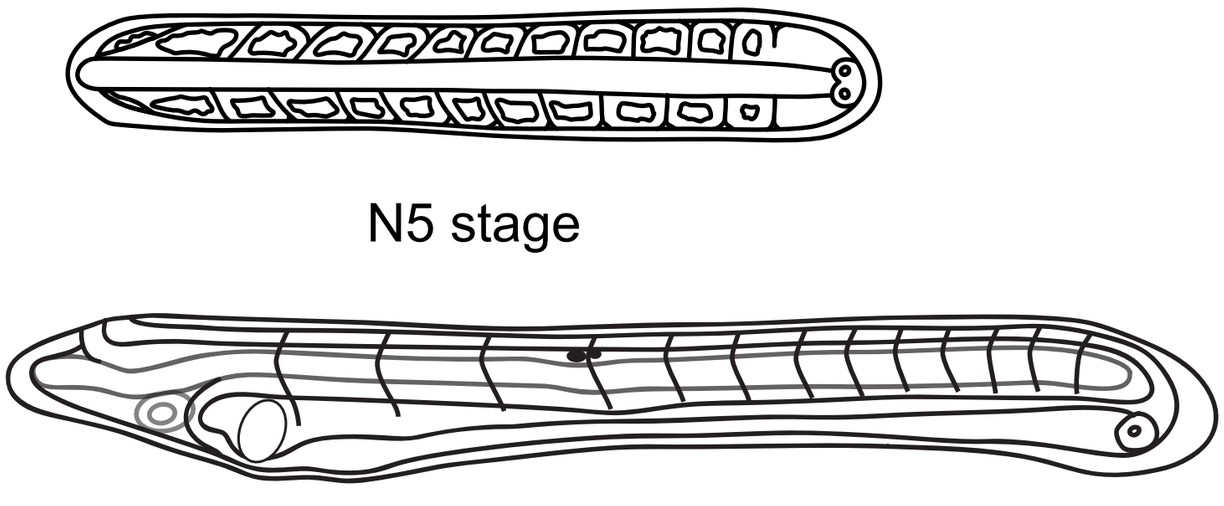

T1 stage

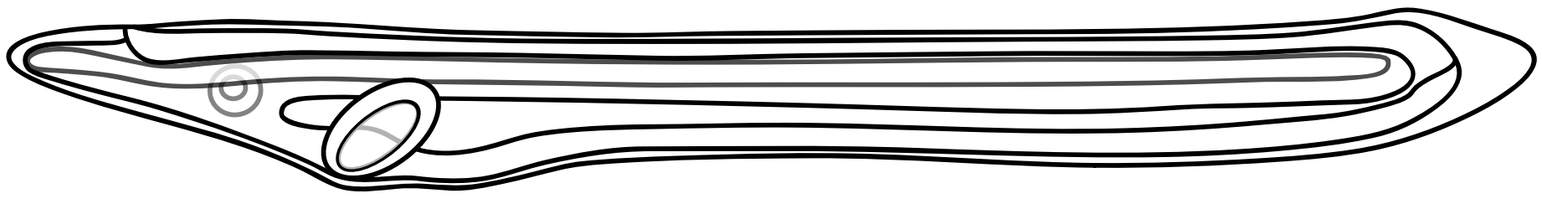

L0 stage

A

Egg
8-cell stage
64-cell stage
128-cell stage
B stage
G1 stage
G1 stage blastopore view
G4 stage
G4 stage blastopore view
G6 stage
G6 stage blastopore view

B. lanceolatum
B. floridae
B. belcheri
B. japonicum
A. lucayanum

100 µm

B

N1 stage
N1 stage dorsal view
N2 stage
N2 stage dorsal view
N4 stage
N4 stage dorsal view

B. lanceolatum
B. floridae
B. belcheri
B. japonicum
A. lucayanum

100 µm

C

T1 stage
L2 stage

B. lanceolatum
B. floridae
B. belcheri
B. japonicum
A. lucayanum

100 µm

		B. lanceolatum [1]			*B. floridae* [2]		*B. belcheri* [3]	*B. japonicum* [4]	*A. Lucayanum* [5]
Stage	**Key feature**	***at 16ºC***	***at 19ºC***	***at 22ºC***	***at 25ºC***	***at 30ºC***	***at 23ºC-24ºC***	***at 25ºC***	***at 27ºC***
1-cell stage	fertilized egg								
2-cell stage	2 cells		1h		45'	30'	45'	50'-1h	1h-1h30' *
4-cell stage	4 cells		1h30'		1h	50'	1h	1h10'	2h-2h30' *
8-cell stage	8 cells		2h		1h30'	1h	1h20'	1h35'	2h-2h30' *
16-cell stage	16 cells		2h30'		2h	1h15'	1h45'	1h55'	3h-3h30' *
32-cell stage	32 cells		3h		2h15'	1h30'	2h10'	2h15'	3h-3h30' *
64-cell stage	64 cells		3h30'		2h30'	1h45'	2h30'	2h35'	4h-4h30' *
128-cell stage	128 cells		4h		3h	2h	2h50'	3h10'	4h-4h30' *
B stage	initiation of asynchronous cell division		4h30'		4h	2h30'		3h20'	5h
G0 stage	initial flattening of the vegetal zone		5h				3h30'		
G1 stage	flattened vegetal pole		6h		4h30'	3h30'		3h40'	
G2 stage	invaginated vegetal pole		7h					4h10'	
G3 stage	cap shaped		8h		5h	4h	3h55'	5h35'	
G4 stage	cup shaped	15h	9h		6h	4h30'		6h-6h20'	9h
G5 stage	vase shaped		10h				5h45'	7h40'	
G6 stage	bottle shaped		11h		6h30'	5h	7h55'	8h50'	
N0 stage	no somite pairs, neural plate	19h	12h	9h			8h30'		12h
N1 stage	1-3 somite pairs	23h	15h	12h	8h30'	6h	10h20'	10h30'	15h
N2 stage	4-5 somite pairs, hatching	27h	18h		9h30'	6h30'	12h	13h	19h
N3 stage	6-7 somite pairs	31h	21h	13h30'					
N4 stage	8-9 somite pairs, prior to schizocoelic somite formation	35h	24h	16h30'	10h30'	7h30'		18h	
N5 stage	10-11 somite pairs	47h	27h	19h30'					32h
T0 stage	12 somite pairs, tailbud shape, enlarged pharyngeal region	51h	30h	27h					
T1 stage	13 somite pairs, mouth and pre-oral pit anlagen, first pigment spot		36h	30h	20h/24h	12h/17h		24h	50h
L0 stage	no gill slits, open mouth		42h		30h	21h			
L1 stage	1 gill slit		48h		32h/36h	23h/28h		36h	72h
L2 stage	2 gill slits				42h/72h	36h	36h/48h	48h	
Ln stage	n gill slits								

Table 1